J. Fluid Mech. (1966), *vol.* 26, *part* 1, *pp.* 69–79
Printed in Great Britain

Flow through a rapidly rotating conduit of arbitrary cross-section

By G. S. BENTON AND D. BOYER†
Department of Mechanics, The Johns Hopkins University, Baltimore

(Received 23 December 1965)

The problem of flow through rotating channels of almost arbitrary cross-section is considered. It is shown that when the ratio of the Rossby number and the Reynolds number is small ($\epsilon = Ro/Re \ll 1$) and when the Reynolds number is not too large ($Re \ll \epsilon^{-1}$): (1) the viscous effects are important only in thin boundary layers along the channel walls; (2) the flow in the interior is geostrophic; and (3) the inertia effects may be neglected everywhere. Solutions for the geostrophic region and the boundary layers are obtained and are combined to give the complete velocity field. Experimental results for a circular conduit are presented which are in good agreement with the theory.

1. Introduction

A problem which has long been of interest in fluid mechanics is that of the laminar flow of a homogeneous incompressible fluid through channels of various cross-sections. Hagen in 1839 and Pousseille in 1840 studied the flow through a circular channel. Their solution is the classical parabolic velocity profile.

A new régime of problems arises if the channel flow occurs in a non-inertial system (in particular, a rotating system). Barua (1954) and Benton (1956) studied the flow through a circular channel rotating at a constant angular velocity about an axis perpendicular to the channel. The differential equations governing this motion are non-linear and intractable. Benton and Barua simplified the differential equations by assuming small angular velocities; their solutions are perturbations on the Hagen–Pousseille flow.

A similar physical system was considered in the present study, but the differential equations were simplified by assuming large rotation rates. In order to gain some physical insight into such channel flows, a series of experiments was conducted. The experiments consisted of pumping water through channels mounted horizontally on a table rotating rapidly around a vertical axis. The flow was then observed by injecting a tracer into the fluid.

A time exposure of an experiment using a channel of circular cross-section is shown. Figure 1 (*b*) (plate 1) was taken with a camera pointing upstream along the axis of the tube. The boundary layers around the periphery of the channel are clearly visible. Fluid in these boundary layers moves towards the point P as indicated in the schematic drawing.

† Now at the Department of Civil Engineering, University of Delaware, Newark, Delaware.

These flows are analogous to an Ekman boundary layer. At P the boundary layers converge. As the boundary layers approach this point, however, their mass flow diminishes steadily: throughout the entire depth of the channel, fluid moves out of the boundary region and back across the conduit. Figure 1 (*b*) (plate 1) seems to indicate that this return flow is concentrated in a 'jet' across the centre of the tube. However, this is not the case: the return flow occurs uniformly within the entire region of free-stream flow, as shown in figure 1 (*a*) (plate 1). This was demonstrated experimentally in several ways: for example, a vertical line of tracer moved across the tube without change of shape or orientation. The concentration of tracer across the centre of the channel in figure 1 (plate 1) seems to be caused by the slightly larger density of the tracer fluid.

Similar results are observed in rapidly rotating channels with different cross-sectional shapes. That is, qualitatively the flow consisted of an axial transport, with well-developed boundary layers occurring along the channel walls and a weak horizontal return flow occurring across the interior.

The structure of such boundary-layer flows can be developed theoretically. In the following discussion, a solution will first be obtained for an almost arbitrary cross-section. Following this, simplified solutions for conduits of symmetric cross-section will be developed. As an example, the solution for the circular cross-section will be examined in some detail. The resulting solutions are similar in many ways to those presented by Hsueh (1965) who studied flow over a corrugated bottom in a laterally unbounded system. However, the solutions discussed by Hsueh are limited to corrugations of small slope, whereas in the present study the slope of the boundary may be finite.

In the boundary-layer solutions for flow through a conduit, examined below, singularities exist at points where the channel walls are parallel to the axis of rotation. Although the fluid velocities may become arbitrarily small in the vicinity of the singularity, the boundary-layer solution is not valid in the immediate vicinity of this point. This does not seem to be of critical physical importance for a point singularity; however, the situation is different when the channel walls are parallel to the axis of rotation over a finite length. To avoid this difficulty, cross-sections which have a finite part of their boundaries parallel to the axis of rotation are excluded from the present discussion.

2. The governing differential equations

It is well known that the equations of motion of a homogeneous incompressible fluid in laminar steady-state flow relative to a set of rectangular Cartesian co-ordinates (x, y, z) rotating at a constant angular velocity $\boldsymbol{\omega}$ with respect to an inertial system are

$$(\mathbf{v}.\nabla)\mathbf{v} = -\nabla\Phi - 2\boldsymbol{\omega}\times\mathbf{v} + \nu\nabla^2\mathbf{v}, \tag{2.1}$$

where

$$\Phi = \tfrac{1}{2}\omega^2 a^2 + (p/\rho) + \phi.$$

Here $\mathbf{v}(u, v, w)$ is the Eulerian velocity; a, the perpendicular distance from the axis of rotation; p, the pressure; ρ, the density; and ϕ the gravitational potential. The equation for conservation of mass is

$$\nabla.\mathbf{v} = 0. \tag{2.2}$$

Choose the z-direction to be parallel to the channel axis and assume that all of the dependent variables, except Φ, are independent of z. Thus Φ must be a linear function of z; i.e. $\Phi_z = -\alpha$, where α is a constant.

Choose the y-axis to be parallel to the axis of rotation and introduce the following dimensionless quantities:

$$(x^*, y^*, z^*) = \left(\frac{x}{S}, \frac{y}{S}, \frac{z}{S}\right), \quad (u^*, v^*, w^*) = \left(\frac{u}{W}, \frac{v}{W}, \frac{w}{W}\right), \quad \Phi^* = \frac{\Phi}{2\omega W S},$$

where S is the maximum vertical dimension of the channel and W is a characteristic speed in the z-direction. Introduce the stream-function defined by the equations

$$u^* = -\psi_y, \quad v^* = \psi_x.$$

Equation (2.2) is thus identically satisfied.

Substituting into (2.1), and eliminating the variation of the total pressure in the (x, y)-plane, one obtains the z-component of the vorticity equation

$$\epsilon Re \frac{\partial(\psi, \nabla^2\psi)}{\partial(x, y)} = w_y + \epsilon\nabla^4\psi, \tag{2.3}$$

and the z-momentum equation

$$\epsilon Re \frac{\partial(\psi, w)}{\partial(x, y)} = \alpha_0 - \psi_y + \epsilon\nabla^2 w, \tag{2.4}$$

where

$$Re = WS/\nu, \quad \epsilon = \nu/(2\omega S^2),$$

and where α_0 is a new constant. Note that, for convenience, the asterisks have been dropped from the dimensionless quantities.

The boundary conditions on the dependent variables ψ and w are

$$\psi(\text{walls}) = \psi_n(\text{walls}) = w(\text{walls}) = 0, \tag{2.5}$$

where n is the derivative taken normal to the wall.

3. Scaling of the flow field

If the angular velocity of the rotating system is made arbitrarily large, the non-dimensional parameter ϵ can be made arbitrarily small for any real fluid and for any conduit of finite size. Let us assume that, mathematically, ϵ is infinitesimal. For the physical problem we wish to consider, let us investigate what restrictions must be placed on other physical parameters.

Let the Reynolds number Re be of order of magnitude ϵ^q. In the interior of the flow field, away from all boundaries, it will be assumed that increments of dependent variables are of the same order as the variables themselves. It will also be assumed that the non-dimensional increment of length in the cross-channel direction, δx, is of the order ϵ^r, where $r \leqslant 0$. As will be noted below, this places some restriction on the shape of the channel to be considered. In physical space, all characteristic lengths which describe variations of the boundary in the x-direction must be of a scale which is equal to or greater than the depth of the channel.

In the interior, let w and ψ be written w_I and ψ_I, and assume that these variables can be expressed as power series in ϵ. The leading terms are

$$w_I = w_0 \epsilon^0, \quad \psi_I = \psi_0 \epsilon^p,$$

where w_0 and ψ_0 are the order of unity, p is unspecified, and the fact that w_I is of the order ϵ^0 follows from the method of non-dimensionalization.

Let us now require that in the interior the effect of friction is unimportant and the flow is geostrophic (i.e. the inertial terms are negligible). This implies from (2.4) that $p < 1$ and $q > -1$. From (2.3) it also follows that $p > 0$. Thus

$$0 < p < 1, \quad q > -1.$$

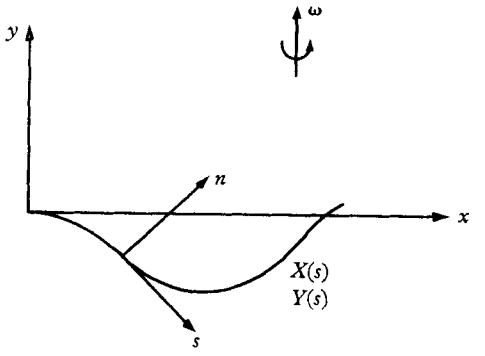

FIGURE 2. Natural co-ordinate system for boundary-layer equations.

In the interior the governing differential equations become

$$w_{0y} = 0, \quad \epsilon^p \psi_{0y} = \alpha_0, \tag{3.1}$$

which implies that α_0 is a constant of order ϵ^p. These equations have the solutions

$$w_0 = g(x), \quad \psi_0 = \alpha_{1y} + f(x), \tag{3.2}$$

where $\alpha_0 = \epsilon^p \alpha_1$ and where the functions $g(x)$ and $f(x)$ are to be determined.

Obviously, (3.2) cannot be made to satisfy the no-slip boundary conditions. We thus conclude that, if approximate solutions of (2.3) and (2.4) exist for the range of values of ϵ and Re we are considering, they must be of the boundary-layer type; that is, near the channel walls normal derivatives must be of different order than ϵ^0. To investigate this problem, one may introduce the natural co-ordinate system shown in figure 2. For a thin boundary in the vicinity of the wall, one can readily transform equations (2.3) and (2.4) into the (s, n) co-ordinate system. When this is done, the slope of the boundary and the radius of curvature of the boundary appear as parameters.

Assume the following relationships, which are characteristic of boundary layers near the regular boundaries:

(i) $\partial/\partial s \sim \epsilon^a$ $(a \geqslant 0)$;

(ii) $\partial/\partial n \sim \epsilon^{-b}$ $(b > 0)$;

(iii) $R \sim \epsilon^c$ $(c \leqslant 0)$;

(iv) Slope of wall $\neq$ infinite;

where R is the radius of curvature of the wall. Under such circumstances the governing differential equations become (after neglecting terms which are obviously of higher order):

$$\left.\begin{aligned} \epsilon Re \frac{\partial(\psi, \psi_{nn})}{\partial(s,n)} &= \frac{dX}{ds} w_n + \epsilon \psi_{nnnn}, \\ \epsilon Re \frac{\partial(\psi, w)}{\partial(s,n)} &= \alpha_1 \epsilon^p - \frac{dX}{ds} \psi_n + \epsilon w_{nn}, \end{aligned}\right\} \tag{3.3}$$

where $X = X(s)$, $Y = Y(s)$ are the parametric equations for the channel wall. Provided friction is important in the boundary layer, the previous restrictions on p and q ensure that the inertia terms are negligible in both of these equations, and that there must be a balance between the friction and Coriolis terms in (3.3). This yields the relations

$$-b = 1+p-4b, \quad \text{and} \quad p-b = 1-2b,$$

respectively, which require that $b = \frac{1}{2}$ and $p = \frac{1}{2}$.

These results can be summarized briefly. The shape of the channel is restricted to a cross-section in which the channel wall is parallel to the axis of rotation at no more than two points; furthermore, the characteristic length scale for undulations of the boundary in the x-direction shall not be of a smaller order of magnitude than the depth of the channel. In this system, the Reynolds number is of the order of magnitude ϵ^q, where $q > -1$. These restrictions make it reasonable to expect a solution in which the flow is geostrophic in the interior and in which the effects of inertia are negligible in the boundary layers. The governing differential equations are linear and are tractable.

4. The velocity field in a conduit of arbitrary cross-section

As noted previously, the solutions for the axial velocity and for the stream-function in the interior geostrophic region are

$$w_0 = g(x), \quad \psi_0 = \alpha_1 y + f(x), \tag{4.1}$$

where $w_I = w_0 \epsilon^0$; $\psi_I = \psi_0 \epsilon^{\frac{1}{2}}$; and where $f(x)$ and $g(x)$ are to be determined. To evaluate the velocity distributions in the boundary layers, let us set up the co-ordinates shown in figure 3. The upper portion of the boundary (subscript 2) and the lower portion of the boundary (subscript 1) are separated by the points P and P', at the extreme positions in the x-direction. It should be noted that P and P' need not be at the same vertical co-ordinate. At these extreme points the wall of the conduit may be parallel to the axis of rotation, as shown at P', or there may be a sharp angle in the wall, as at P. The equations of the two bounding surfaces may be expressed in parametric form as

$$\left.\begin{aligned} X_1 = X_1(s_1), \quad X_2 = X_2(s_2), \\ Y_1 = Y_1(s_1), \quad Y_2 = Y_2(s_2). \end{aligned}\right\} \tag{4.2}$$

In the vicinity of the upper and lower boundaries, write

$$\left.\begin{aligned} w_B &= w_0 \epsilon^0 + w^{(i)} \epsilon^0, \\ \psi_B &= \psi_0 \epsilon^{\frac{1}{2}} + \psi^{(i)} \epsilon^{\frac{1}{2}}, \end{aligned}\right\} \tag{4.3}$$

where the subscript B indicates that the variables are evaluated in a boundary layer, and the superscript i denotes boundary 1 or 2. It is clear that at the outer edge of the boundary layer $w^{(i)}$ and $\psi^{(i)}$ must vanish.

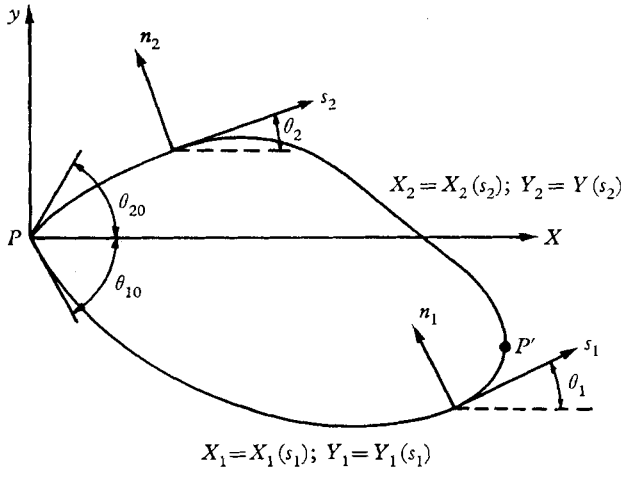

FIGURE 3. Natural co-ordinates for boundary-layer equations in channel of irregular shape.

After substituting (4.1) and (4.3) into the boundary-layer equations (3.3), one obtains

$$\left.\begin{aligned} \psi^{(i)}_{n_i n_i n_i} + (dX_i/ds_i)\, w^{(i)}_{n_i} &= 0, \\ w^{(i)}_{n_i n_i} - (dX_i/ds_i)\, \psi^{(i)}_{n_i} &= 0. \end{aligned}\right\} \tag{4.4}$$

Solutions of these equations which satisfy the no-slip condition at the lower boundary are

$$\left.\begin{aligned} \psi_B &= \psi_0(s_1)\,\epsilon^{\frac{1}{2}}\left[1-\exp\left[-n_1\left(\frac{1}{2}\frac{dX_1}{ds_1}\right)^{\frac{1}{2}}\right]\left\{\sin\left[n_1\left(\frac{1}{2}\frac{dX_1}{ds_1}\right)^{\frac{1}{2}}\right]+\cos\left[n_1\left(\frac{1}{2}\frac{dX_1}{ds_1}\right)^{\frac{1}{2}}\right]\right\}\right], \\ w_B &= w_0(s_1)+\psi_0(s_1)\left(2\frac{dX_1}{ds_1}\right)^{\frac{1}{2}}\exp\left[-\left(\frac{1}{2}\frac{dX_1}{ds_1}\right)^{\frac{1}{2}}\right]\cos\left[n_1\left(\frac{1}{2}\frac{dX_1}{ds_1}\right)^{\frac{1}{2}}\right], \end{aligned}\right\} \tag{4.5}$$

where

$$w_0(s_1)+\psi_0(s_1)\,(2\,dX_1/ds_1)^{\frac{1}{2}} = 0. \tag{4.6}$$

The corresponding solutions for the upper boundary are

$$\left.\begin{aligned} \psi_B &= \psi_0(s_2)\,\epsilon^{\frac{1}{2}}\left[1+\exp\left[n_2\left(\frac{1}{2}\frac{dX_2}{ds_2}\right)^{\frac{1}{2}}\right]\left\{\sin\left[n_2\left(\frac{1}{2}\frac{dX_2}{ds_2}\right)^{\frac{1}{2}}\right]-\cos\left[n_2\left(\frac{1}{2}\frac{dX_2}{ds_2}\right)^{\frac{1}{2}}\right]\right\}\right], \\ w_B &= w_0(s_2)-\psi_0(s_2)\left(2\frac{dX_2}{ds_2}\right)^{\frac{1}{2}}\exp\left[n_2\left(\frac{1}{2}\frac{dX_2}{ds_2}\right)^{\frac{1}{2}}\right]\cos\left[n_2\left(\frac{1}{2}\frac{dX_2}{ds_2}\right)^{\frac{1}{2}}\right], \end{aligned}\right\} \tag{4.7}$$

where

$$w_0(s_2)-\psi_0(s_2)\,(2\,dX_2/ds_2)^{\frac{1}{2}} = 0. \tag{4.8}$$

The conditions (4.6) and (4.8) are expressed, respectively, in terms of the parameter s_1 and s_2 along the lower and upper boundaries. It is convenient to re-cast these equations in terms of the independent variable x. Let us write

$$\left.\begin{aligned} dX_1/ds_1 &= \cos\{\theta_1(x)\}, & dX_2/ds_2 &= \cos\{\theta_2(x)\}, \\ Y_1(s_1) &= \overline{Y}_1(x), & Y_2(s_2) &= \overline{Y}_2(x), \end{aligned}\right\} \tag{4.9}$$

where $\overline{Y}_1$ and $\overline{Y}_2$ are the new functional forms of Y_1 and Y_2. Then, in terms of x, the conditions (4.6) and (4.8) become

$$\left.\begin{aligned} g(x)+\{\alpha_1\overline{Y}_1(x)+f(x)\}\{2\cos[\theta_1(x)]\}^{\frac{1}{2}} &= 0,\\ g(x)-\{\alpha_1\overline{Y}_2(x)+f(x)\}\{2\cos[\theta_2(x)]\}^{\frac{1}{2}} &= 0,\end{aligned}\right\} \tag{4.10}$$

respectively.

The solutions for the unknown functions $f(x)$ and $g(x)$ are therefore

$$\left.\begin{aligned} f(x) &= -[\alpha_1\{\overline{Y}_2(\cos\theta_2)^{\frac{1}{2}}+\overline{Y}_1(\cos\theta_1)^{\frac{1}{2}}\}]/[(\cos\theta_1)^{\frac{1}{2}}+(\cos\theta_2)^{\frac{1}{2}}],\\ g(x) &= [\alpha_1(\overline{Y}_2-\overline{Y}_1)\,(2\cos\theta_1\cos\theta_2)^{\frac{1}{2}}]/[(\cos\theta_1)^{\frac{1}{2}}+(\cos\theta_2)^{\frac{1}{2}}].\end{aligned}\right\} \tag{4.11}$$

These functions, when substituted into (4.1), specify the complete solution for the velocity field far away from the boundaries. Substitution of (4.1) into (4.5) and (4.7) specifies the flow in the boundary layers.

It is to be noted that in the interior the flow across the channel (u component) is a constant. However, the axial flow and the vertical component of the velocity may be functions of the x-co-ordinate.

The solutions are not valid in the immediate neighbourhood of points P and P', as shown in figure 3. It is important, however, to ascertain whether these solutions call for velocities which are arbitrarily small, finite but non-zero, or infinite in the vicinity of these two points. In the latter case, especially, a question could be raised concerning the effect of the singularities.

It has not been possible to develop a full solution for the stream-function and the axial component of the flow in the vicinity of the two singularities. However, it would certainly be desirable to ensure that the vertical component v does not become indefinitely large in the neighbourhood of P and P'. Consider the neighbourhood of a singularity P, as shown in figure 3. The two angles θ_{20} and θ_{10} may or may not be equal, and either or both may be right angles. In the neighbourhood of P

$$f(x) \sim -\alpha_1\frac{x(\tan\theta_{20})\,(\cos\theta_{20})^{\frac{1}{2}}+x(\tan\theta_{10})\,(\cos\theta_{10})^{\frac{1}{2}}}{(\cos\theta_{20})^{\frac{1}{2}}+(\cos\theta_{10})^{\frac{1}{2}}}, \tag{4.12}$$

and therefore

$$v_0 = \frac{\partial f}{\partial x} \sim -\alpha_1\frac{(\tan\theta_{20})\,(\cos\theta_{20})^{\frac{1}{2}}+(\tan\theta_{10})\,(\cos\theta_{10})^{\frac{1}{2}}}{(\cos\theta_{20})^{\frac{1}{2}}+(\cos\theta_{10})^{\frac{1}{2}}}. \tag{4.13}$$

It is to be noted that v_0 tends to become infinite in the neighbourhood of P if one of the two angles θ_{10} and θ_{20} is a right angle. To exclude this possibility, certain cross-sectional shapes (such as a semicircle) must be excluded.

5. Physical discussion and example

The physical interpretation of the general solution presented in the preceding section is straightforward. In the interior, the flow is geostrophic. This does not exclude, however, the possibility of variation of the v and w components of the flow in the x-direction. To the order of accuracy considered, such velocity shears will result in negligible friction and inertial effect.

The value of the functions $v(x)$ and $w(x)$ are determined in the lower and upper boundary layers. The axial component of the flow $w(x)$ is specified by the rate of

variation of the total pressure in the x-direction. If this quantity is to be a function of the x-co-ordinate alone, then the quantity Φ_x must be the same throughout the entire depth of the channel. This quantity is, however, associated with the mass transport in the x-direction in each boundary layer. If the drop in Φ in the upper boundary layer is to be compatible with the drop in Φ in the bottom boundary layer, there must in general be a transfer of fluid from one boundary layer to another in order to appropriately adjust the mass flows. Thus, both $w(x)$ and $v(x)$ are determined by the boundary-layer solution.

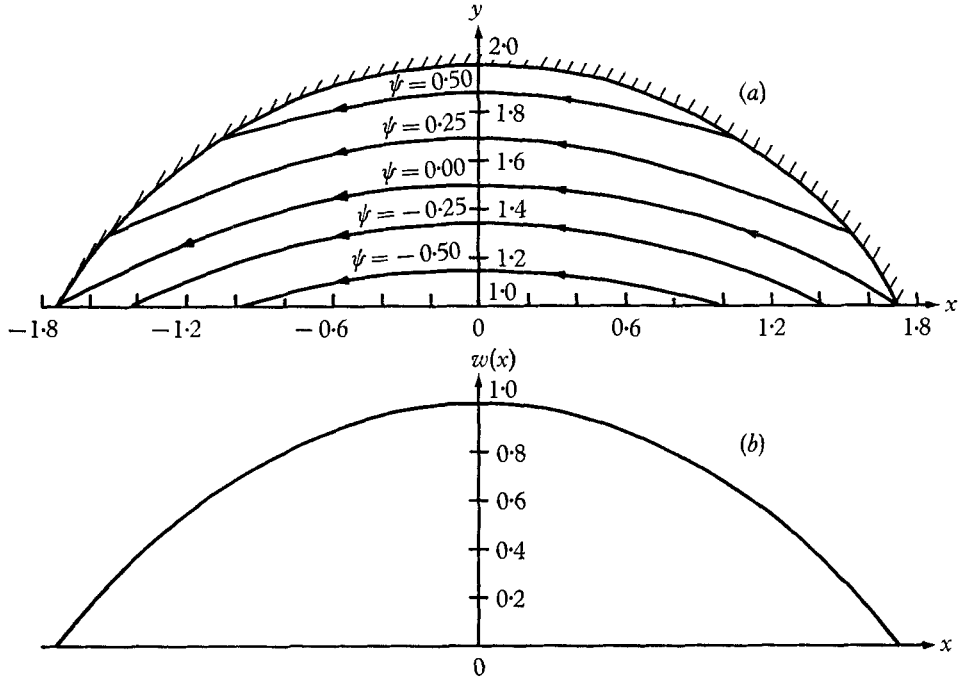

FIGURE 4. Flow through tube with plane bottom and cylindrical top: (*a*) streamlines in cross-section outside of boundary layers; (*b*) axial velocity $w(x)$ in free stream.

Let us now apply the equations to a particular example. Consider the channel shown in figure 4 (*a*), in which the upper boundary is a portion of a circular arc of radius 2 and the lower boundary is horizontal and perpendicular to the axis of rotation. For this case, the various pertinent functions are

$$\left.\begin{aligned} \overline{Y}_1 = 1, \quad \overline{Y}_2 = \sqrt{(4-x^2)}, \\ \cos\theta_1 = 1, \quad \cos\theta_2 = \tfrac{1}{2}\sqrt{(4-x^2)}. \end{aligned}\right\} \tag{5.1}$$

This yields, for the interior

$$\left.\begin{aligned} \psi_0 &= \frac{\sqrt{2}y - \sqrt{2}\{(4-x^2)^{\frac{3}{4}} + \sqrt{2}\}}{(4-x^2)^{\frac{1}{4}} + \sqrt{2}}, \\ w_0 &= \frac{2(4-x^2)^{\frac{1}{4}}\{(4-x^2)^{\frac{1}{2}} - 1\}}{(4-x^2)^{\frac{1}{4}} + \sqrt{2}}, \end{aligned}\right\} \tag{5.2}$$

where α_1 has been determined by normalizing on the axial velocity component at $x = 0$. Recall that ψ in the interior is given by $\psi_I = \epsilon^{\frac{1}{2}}\psi_0$. The velocity distributions in the upper and lower boundary layers can readily be determined, but are not reproduced here. The interior stream-function and axial velocity component are plotted in figure 4.

6. Channels with symmetric cross-sections

Conduits which are symmetrical in the y-co-ordinate are of particular interest. One reason for this, of course, is the fact that the lower half of such a conduit approximates the conditions of flow through an open channel with a horizontal free surface on which there are no shearing stresses. This approximation involves negligible error in the case of geophysical applications, in which the centrifugal force due to the earth's rotation is compensated for by the oblateness of the earth and therefore does not explicitly enter the definition of Φ.

For a symmetric cross-section

$$\overline{Y}_2 = -\overline{Y}_1, \quad \theta_2 = -\theta_1. \tag{6.1}$$

Thus, as a result of the symmetry, the vertical velocity v_0 is identically equal to zero and the components u_0 and w_0 are given by

$$u_0 = -\alpha_1, \quad w_0 = -\alpha_1(2\cos\theta_1)^{\frac{1}{2}}\overline{Y}_1. \tag{6.2}$$

It should be noted that, if θ_1 is small, $\cos\theta_1 \approx 1$ and the axial velocity w_0 is approximately proportional to the elevation at the bottom $\overline{Y}_1$. This is in accord with the theory for flow over corrugated bottoms with small slope, developed by Hsueh (1965).

In the vicinity of the lower boundary, the solution is given by (4.5). Near the upper boundary, the velocity distribution as given by (4.7) is similar but inverted.

As an example, consider a conduit with circular cross-section. The pertinent functions are

$$\overline{Y}_1 = -\sqrt{(\tfrac{1}{4} - x^2)}, \quad \cos\theta_1 = \sqrt{(1 - 4x^2)}, \tag{6.3}$$

which yields for the flow in the interior

$$\psi_0 = \sqrt{2}y, \quad w_0 = \{1 - 4x^2\}^{\frac{3}{4}}, \tag{6.4}$$

where α_1 is again eliminated by normalizing on the axial velocity component at $x = 0$. This distribution is presented in figure 5, where it is compared with experimental data.

7. Experimental studies of flow through a circular conduit

The validity of the above theory can readily be tested by examining the distribution of axial velocity of a fluid moving through a conduit of circular cross-section. In such a study the existence of boundary layers can also be qualitatively verified.

A plastic pipe 7·62 cm (3 in.) in diameter was used. The pipe, water reservoirs, and pump were placed on a rotating table. The water temperature varied from about 21 to 26 °C, and rates of rotation of 8 to 18 revolutions per minute were

employed. The value of ϵ varied from $4{\cdot}5 \times 10^{-5}$ to $1{\cdot}0 \times 10^{-4}$. The Reynolds number was also scaled appropriately. For the theory to be applicable, it is required that $Re \ll \epsilon^{-1}$, or alternatively, in terms of the Rossby number, $Ro = W/2\omega S \ll 1$. This was achieved by restricting the speed of the axial flow. In the experiments the maximum velocity W_0 varied from 0·76 to 0·88 cm/sec, and the Rossby number varied from $2{\cdot}7 \times 10^{-2}$ to $6{\cdot}2 \times 10^{-2}$.

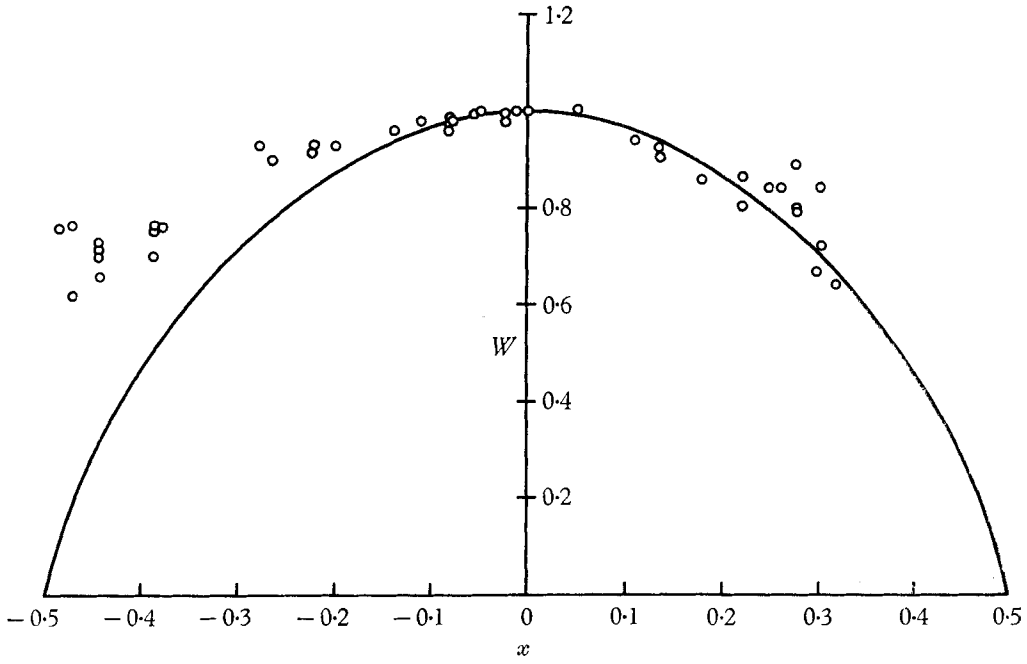

FIGURE 5. Measurements of axial velocity across the axis of a rotating cylindrical tube. Theoretical distribution entered as solid curve. Theory calls for errors of the order of 10 % or larger for $|x| > 0{\cdot}27$.

Ten series of measurements of the lateral distribution of axial velocity were made by injecting dye into the fluid at various positions across the pipe and by measuring the axial motion of the dye from photographs. The results are shown in figure 5. The profile of the observed axial velocities follows the theory very closely near the centre of the pipe. Differences are, however, observed near the lateral boundaries where the pipe wall becomes parallel to the axis of rotation.

This is, of course, not surprising in view of the singularities which exist at these points. The theory as presented assumes that in equation (3.3) $dX/ds \gg \epsilon^{\frac{1}{2}}$ and also that $dX/ds \gg Ro$. Using values of ϵ and Ro from the experiment, one obtains the requirement that $\cos\theta \gg 0{\cdot}06$, where θ is the slope of the boundary. Thus, the theory should not be very satisfactory for $\cos\theta < 0{\cdot}6$, or $53° < \theta < 127°$. This corresponds to $|x| = 0{\cdot}4$, a value close to that at which the observed data become significantly different from the theoretical predictions. It should also be noted that the observed deviations are not symmetric across the channel: a result which would be characteristic of the effects of the non-linear inertial terms. The high axial velocities for $x < -0{\cdot}3$ are probably associated with the advection of

large central velocities toward the tube boundary by the cross-flow. Presumably, if a higher rotation rate were used, and the Rossby number and ϵ were reduced accordingly, the theory would be valid over an increasing portion of the pipe. This could not be achieved, however, with the available turntable.

In general, the results of the experiments show that the observed distribution of axial velocities are not too different from those predicted. While this cannot be regarded as complete verification of the theory, the results are encouraging.

The research presented in this paper was supported by the National Science Foundation, under Grant GP-1892. The assistance of Mr Gerald Putland in conducting the laboratory experiments is also gratefully acknowledged.

REFERENCES

BARUA, S. N. 1954 Secondary flow in a rotating straight pipe. *Proc. Roy. Soc. London* A. **227**, 133–139.

BENTON, G. S. 1956 The effects of the earth's rotation on laminar flow in pipes. *J. Appl. Mech.* **23**, 123–127.

HAGEN, G. 1839 Über die Bewegung des Wassers in engen zylindrischen Rohren. *Pogg. Ann.* **46**, 423.

HSUEH, Y. 1965 Viscous flow over a corrugated bottom in a strongly rotating system. Doctorol dissertation, John Hopkins University.

POUSSEILLE, J. 1840 Recherches expérimentelles sur la mouvement des liquides dans les tubes de très petits diamètres. *C.r. hebd. Séanc Acad. Sci., Paris* **11**, 961 and 1041.

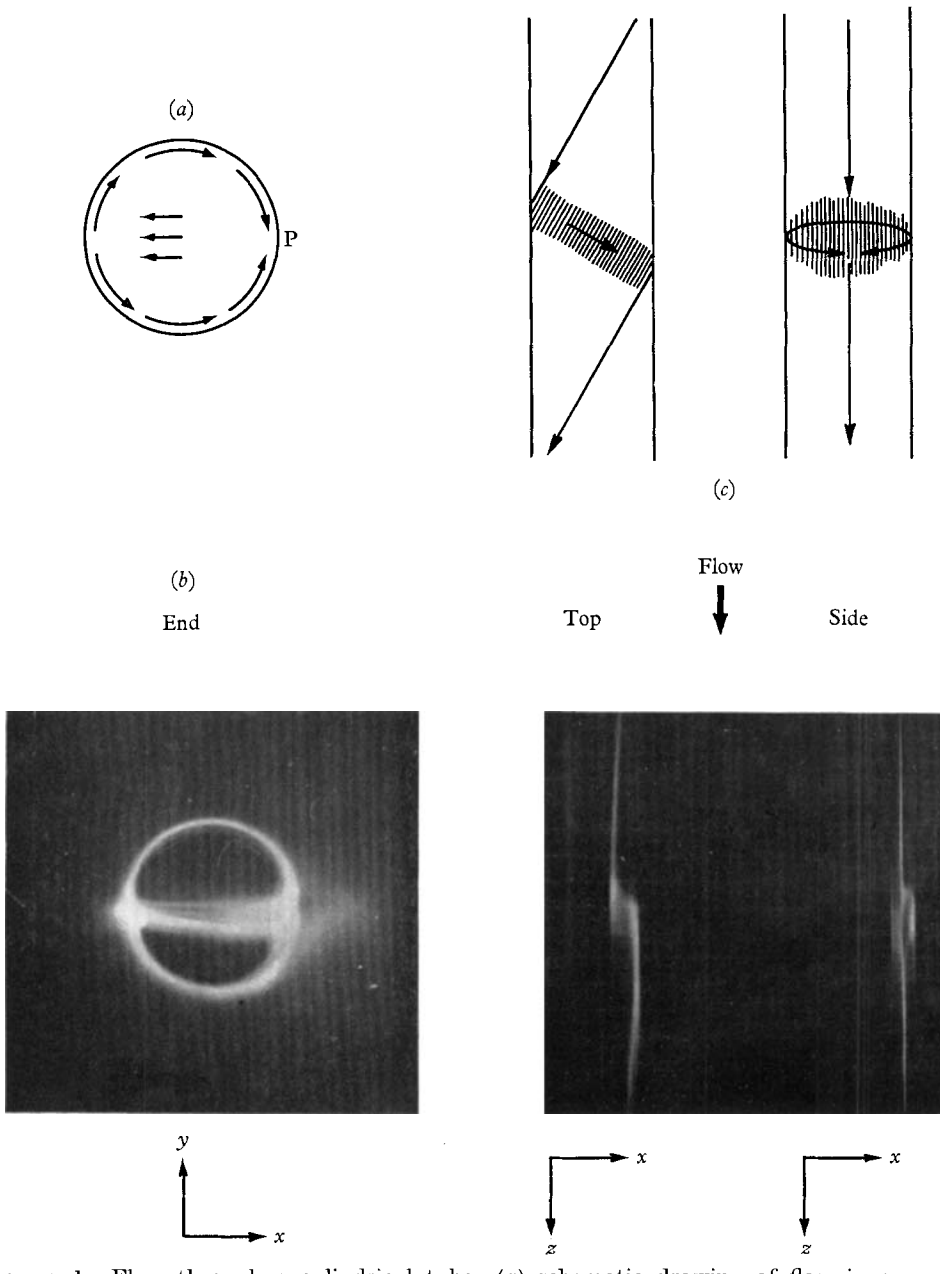

FIGURE 1. Flow through a cylindrical tube: (*a*) schematic drawing of flow in cross-section; (*b*) photograph taken along axis of tube; (*c*) schematic drawings and photographs of top and side views.